DOI: 10.1002/chem.201001749

C_2-Symmetric Chiral Disulfoxide Ligands in Rhodium-Catalyzed 1,4-Addition: From Ligand Synthesis to the Enantioselection Pathway

Ronaldo Mariz,[a] Albert Poater,[b] Michele Gatti,[a] Emma Drinkel,[a] Justus J. Bürgi,[a] Xinjun Luan,[a] Sascha Blumentritt,[a] Anthony Linden,[a] Luigi Cavallo,*[c] and Reto Dorta*[a]

Abstract: A family of chiral C_2-symmetric disulfoxide ligands possessing biaryl atropisomeric backbones has been synthesized by using the Andersen methodology. Complete characterization includes X-ray crystallographic studies of all ligands and some of their rhodium complexes. Their synthesis, optical purity, electronic properties, and catalytic behavior in the prototypical rhodium-catalyzed 1,4-addition of phenylboronic acid to 2-cyclohexen-1-one are presented through an in depth study of this ligand class. Density functional theory calculations on the step of the catalytic cycle that determines the enantioselectivity are presented and reinforce the first hypothetical explanations for the high levels of asymmetric induction observed.

Keywords: asymmetric catalysis · chiral auxiliaries · conjugate addition · enantioselectivity · sulfoxides

Introduction

The increasing demand for enantiomerically pure compounds in many industrial sectors, combined with the need for atom economy and efficiency, has catapulted asymmetric transition-metal catalysis to the forefront of research efforts.[1,2] Among the plethora of chiral ligands developed so far, those possessing a C_2-symmetric axis are often the most successful at inducing high degrees of selectivity in catalysis.[3] The overwhelming majority of these ligands have phosphorus, nitrogen, and oxygen as donor atoms, and only in the last few years have other systems appeared, for example chiral dienes, in combination with rhodium and iridium catalysis.[1b–c,4] An alternative class that has been more sporadically applied in catalysis are ligands that contain sulfur donors.[5] Among these compounds, sulfoxides are especially appealing, owing to their inherent chirality at sulfur, their high optical stability, and their facile synthetic access in enantiomerically pure form.[6] Although, the sulfinyl group has played an important role as an efficient chiral auxiliary in numerous asymmetric transformations, the application of this moiety as a ligand for transition-metal catalysts has remained neglected.[7–10]

We surmised that the combination of a rigid, C_2-symmetric backbone framework and two enantiopure chiral sulfoxide donors would create an efficient chelating ligand environment. The extremely powerful atropisomeric biaryl-type backbones that have been so successful for diphosphine ligands seemed to be an ideal first choice. In contrast to the BINAP-type systems, we also anticipated that the diastereomeric ligands that we would create, when switching achiral phosphine moieties with enantiopure chiral sulfoxides, would allow us to separate the atropisomeric backbone moieties, thus enabling the use of racemic precursor molecules of these fragments (Scheme 1).

To gain access to these ligands we chose Andersen's approach, which involves the nucleophilic addition of an organometallic reagent (organolithium or organogrignard reagent) to a sulfinylating agent containing an electrophilic

[a] R. Mariz, M. Gatti, E. Drinkel, J. J. Bürgi, X. Luan, S. Blumentritt, Dr. A. Linden, Prof. Dr. R. Dorta
Organisch-chemisches Institut
Universität Zürich
Winterthurerstrasse 190, 8057 Zürich (Switzerland)
E-mail: dorta@oci.uzh.ch

[b] Dr. A. Poater
Catalan Institute for Water Research (ICRA)
H2O Building, Scientific and Technological Park
University of Girona
Emili Grahit 101, 17003 Girona (Spain)

[c] Prof. Dr. L. Cavallo
Dipartimento di Chimica
Università degli Studi di Salerno
Via Ponte don Melillo, Fisciano (SA), 84084 (Italy)

The Supporting Information for this article contains all computational and experimental details and is available on the WWW under http://dx.doi.org/10.1002/chem.201001749.

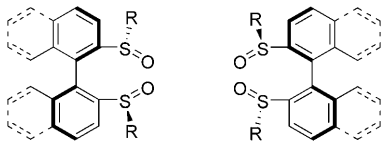

Scheme 1. Disulfoxides with C_2-symmetric backbone.

sulfur atom of known configuration.[11] Based upon previous reports using this approach,[12,13] we have recently shown that two chiral disulfoxide ligands that are analogues of Noyori's BINAP ligand,[14] and its derivative BIPHEMP,[15] can be used successfully as chiral ligands in the rhodium-catalyzed addition of arylboronic acids to α,β-unsaturated carbonyl compounds (Miyaura–Hayashi reaction).[16]

A common pathway for tuning catalytic properties in C_2-symmetric atropisomeric biaryl ligands is the variation of their dihedral angle, induced by changes in the substitution of the backbone units.[17] The modification of geometry and, as a consequence, the electronic distribution around the metal center in many cases alters the activity and/or selectivity of a given catalytic system.[18] Another way to tune catalyst performance of well-established ligand families relies on changes of the stereoelectronic properties (i.e., σ basicity or π acidity) of the groups directly attached to the donor atom. For instance, the difference in donor–acceptor abilities has been investigated for diphosphine ligands and shown to promote significant changes in both activity and selectivity for a given reaction.[19]

Our initial findings on the successful use of two disulfoxide ligands in the Miyaura–Hayashi reaction serve as a basis for the study we report herein. Owing to the novelty of this ligand family, and in line with early studies done on other ligand classes, we wanted to see how the substitution patterns of both the backbone and the sulfoxide groups affect the synthesis of the ligands and their coordination ability to rhodium, as well as their catalytic performance in the prototypical 1,4-addition reaction of phenylboronic acid to 2-cyclohexen-1-one. The results reported below show that the synthesis of these disulfoxides is not always as straightforward as expected. Their coordination ability with respect to electronic ligand modifications is investigated by synthesizing a series of carbonyl-containing rhodium complexes, and the catalytic performance of the respective ligands was compared. Within the context of the selectivity pathway in the Miyaura–Hayashi reaction, preliminary results indicate an unusual mechanism in the enantioselection when employing these atropisomeric disulfoxide ligands. To understand the origin of selectivity, density functional theory (DFT) calculations were performed with the disulfoxide–rhodium systems showing the best selectivity in catalysis and the results are presented here.[20] Further details on the origin of the stereoselectivity by these disulfoxide–rhodium and related catalysts can be found in reference [21].

Results and Discussion

General synthetic strategy: The general synthetic strategy, outlined in (Scheme 2), involves nucleophilic substitution on a sulfinate ester (Andersen method). Starting with backbone

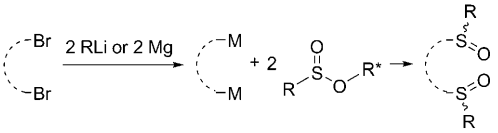

Scheme 2. General synthetic strategy.

molecules containing two bromides, the first reaction with either an organolithium compound or magnesium metal leads to either a dilithiated or di-Grignard derivative. These nucleophiles are then used in consecutive substitution reactions on the sulfinate ester to give the desired products in one synthetic step.

Synthesis of C_2-symmetric backbone precursors: As mentioned above, we wanted to get a clearer picture regarding the behavior of our disulfoxide ligands with respect to modifications of the atropisomeric backbone and selected three well-known structures (Scheme 3) for the present study. The

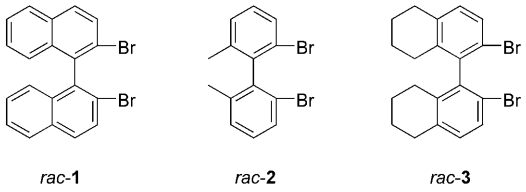

Scheme 3. Well-known structures for the backbone.

racemic dibromo precursors shown are either commercially available (*rac*-**1**),[22] or can be easily synthesized by using established synthetic methods. To access *rac*-**2**, the synthetic pathway developed by Schmid and Frejd was slightly modified.[23] Compound *rac*-**3** was obtained in one step from *rac*-**1** by means of selective partial hydrogenation by using Ru/C.[24]

Synthesis of sulfinate esters: To gain access to electronically modified sulfoxide ligands with similar steric properties that incorporate the parent atropisomeric backbone *rac*-**1**, we trapped racemic sulfinyl chlorides **4**–**9**,[25] with either commercially available diacetone-D-glucose (DAG, Method **A**) or cheap L-menthol (Method **B**), as stereo-controlling alcohols (Scheme 4).

In all cases, the corresponding sulfinates (**10**–**15**) were obtained in good to excellent yields (see the Supporting Information). Some of these sulfinates are known and were synthesized according to the literature procedures [(*S*)-**12** and (*S*)-**13**].[26,27] Sulfinate (*R*)-**13** was purchased and used as re-

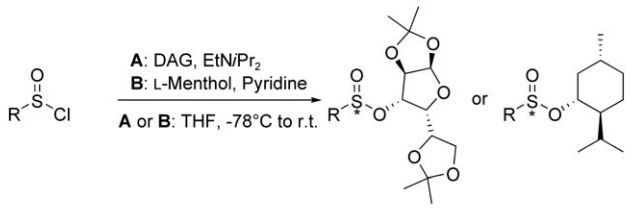

4: R = Ph	**10**: R = Ph	---
5: R = 4-FPh	**11**: R = 4-FPh	---
6: R = Cy	**12**: R = Cy	---
7: R = p-Tol	---	**13**: R = p-Tol
8: R = 4-MeOPh	---	**14**: R = 4-MeOPh
9: R = 4-CF_3Ph	---	**15**: R = 4-CF_3Ph

Scheme 4. Synthesis of DAG and L-menthol sulfinates **10**–**15**.

spectroscopy, analysis of both isomers presented a complex set of signals resulting in no direct assignment of configuration for these sulfinates.

Although (*S*)-**10** and **15** were not obtained as diastereomerically pure compounds, they were nevertheless used for the synthesis of electronically modified disulfoxide ligands below.

Disulfoxide synthesis

Backbone variations: The syntheses of disulfoxides **16**, **17**, and **18** are summarized in Scheme 5. The addition of menthyl sulfinate ester (*S*-**13**) to the dilithiated intermediate derived from *rac*-**1** afforded *p*-Tol-BINASO (**16**), as a pair of diastereomers in approximately 90% yield.[28] The *P* and *M* atropisomers of **16** were easily separated by using silica-gel chromatography. For convenience, we adopt for each disulfoxide ligand a lower case letter after the compound number to indicate the order in which these isomers are collected in the chromatographic purification of their crude reaction mixture. Therefore, **16a** refers to the first compound isolated and **16b** refers to the diastereoisomer collected in later fractions. For unknown reasons, only traces of the desired disulfoxide were formed after the addition of **13** to the dilithiated species of *rac*-**2** (independent of whether *n*BuLi, *n*BuLi/TMEDA, *s*BuLi or *t*BuLi was used). Sulfinate **13** did

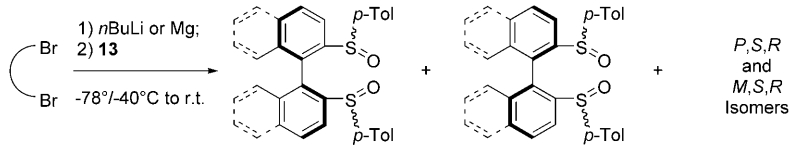

rac-**1**	(*P*,*S*,*S*)-**16a** (45% yield)	(*M*,*S*,*S*)-**16b** (45% yield)	---
rac-**1**	(*P*,*R*,*R*)-**16b'** (38% yield)	(*M*,*R*,*R*)-**16a'** (34% yield)	---
rac-**2**	(*P*,*S*,*S*)-**17a** (28% yield)	(*M*,*S*,*S*)-**17b** (27% yield)	---
rac-**2**	(*P*,*R*,*R*)-**17b'** (28% yield)	(*M*,*R*,*R*)-**17a'** (27% yield)	---
rac-**3**	---	(*M*,*S*,*S*)-**18b** (39% yield)	(*DNHS*)-**18a** (34% yield)

Scheme 5. Synthesis of *p*-Tol-disulfoxides **16**, **17**, and **18**.

ceived. The 4-methoxyphenyl counterpart (*S*)-**14** is also known, but its synthesis was modified to give highly diastereopure material in 63% overall yield.[27] The new sulfinate (*S*)-**11** was formed with high selectivity and the optically pure compound was obtained in 88% yield. Unequivocal determination of the absolute configuration of both (*S*)-**11** and (*S*)-**14** was established by an X-ray diffraction study and their structures are shown in Figure 1. The reaction of phenyl sulfinyl chloride with DAG gave (*S*)-**10** in 98% yield, as a diastereomeric mixture in a 10:1 ratio (*S*:*R*). Unfortunately, column chromatography or recrystallizations from pentane/diethyl ether did not affect the relative amount of the two isomers. Nevertheless, we could establish the major isomer as (*S*)-**10** through single-crystal X-ray studies (Figure 1). The 4-(trifluoromethyl) analogue **15** was obtained in 96% yield as an approximate 3:2 mixture of two diastereoisomers that were separated by column chromatography. In this case, the products were obtained as oils and did not allow crystallographic analysis. Furthermore, using ^{1}H, ^{13}C, and ^{19}F NMR

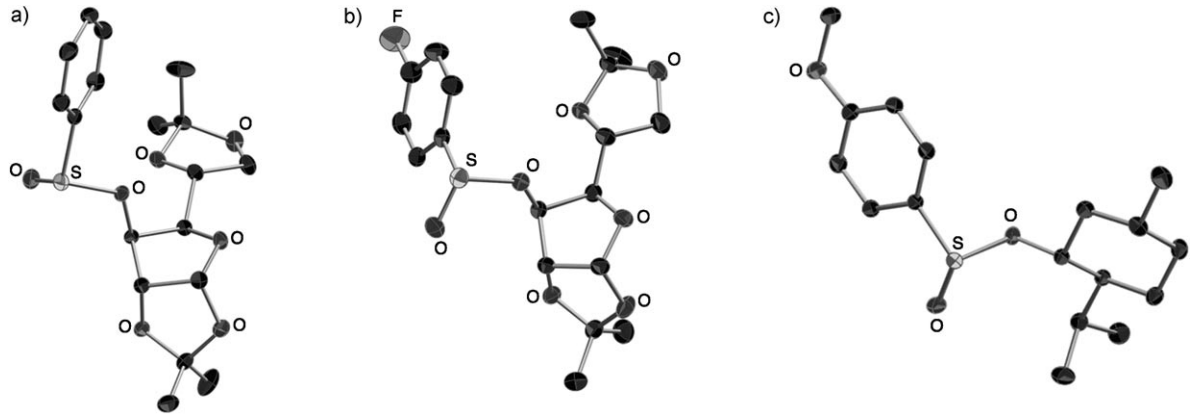

Figure 1. The solid-state molecular structures of *S*-configured sulfinates a) (*S*)-**10**, b) (*S*)-**11**, and c) (*S*)-**14**.

undergo nucleophilic substitution when treated with the di-Grignard derivative of *rac*-**2**. The di-Grignard reagent, however, was exceedingly difficult to generate (see the Supporting Information). Nevertheless, the desired disulfoxide ligand *p*-Tol-MeBIPHESO (**17**) could be obtained in 50–60% overall yield, after separation of the pair of diastereoisomers by column chromatography. Notably, for both *p*-Tol-BINASO and *p*-Tol-MeBIPHESO, we also synthesized the corresponding (*R*)-configured disulfoxides by using commercially available sulfinate (*R*)-**13** and named the respective products **16′** and **17′**.

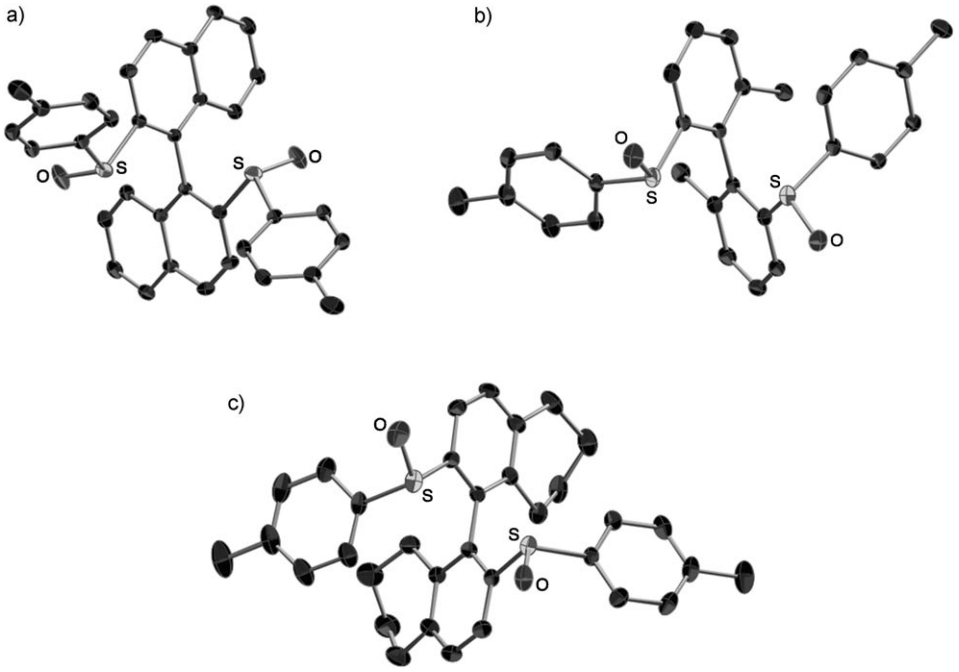

Figure 2. The solid-state molecular structures of a) (*M*,*R*,*R*)-*p*-Tol-BINASO (**16a′**),[16a] b) (*M*,*S*,*S*)-*p*-Tol-MeBIPHESO (**17b**),[16b] and c) (*M*,*S*,*S*)-*p*-Tol-H_8-BINASO (**18b**).

For the third variation of the backbone residue included in our study, as described for H_8-BINAP,[24b] the di-Grignard reagent was obtained upon heating a mixture of *rac*-**3** and magnesium in THF–toluene (1:3) at refluxing temperature. The resulting organometallic species was then allowed to react with **13** at −40 °C and slowly warmed to room temperature. Surprisingly, instead of the expected pair of diastereomers, only one of the diastereoisomers (**18b**) and another compound (**18a**) were formed in 72% overall yield. This byproduct was separated from the predicted diastereoisomer by chromatography and analyzed. A set of two sharp signals of equal intensity around $\delta = 2.5$–2.7 ppm in the ^{1}H NMR spectrum attributed to the methyl groups of the *p*-tolyl fragment, together with a more complicated spectrum in the aromatic region, meant that a set of diastereomers possessing non-homochiral stereogenic sulfur centers (e.g., *M*- or *P*-*S*,*R*, from this point onwards abbreviated *DNHS*) represented the most likely assignment of its structure.

Crystals suitable for X-ray crystallography were obtained for ligands **16a′**, **17b** and **18b** and allowed an unambiguous assignment of all sites of the molecules (Figure 2). Comparison of (*M*,*S*,*S*)-*p*-Tol-H_8-BINASO (**18b**) with its fully conjugated analogue and the biphenyl derivative shows no significant variation in S–O bond distances (1.4922(16) Å for BINASO; 1.4988(16) Å for Me-BIPHESO; 1.495(2) Å for H_8-BINASO).

Sulfinyl group variations: To understand the influence of the substitution pattern at the sulfoxide moiety, the sulfinate esters **10**–**12** and **14**, **15** were incorporated into the backbone framework *rac*-**1** to provide five other disulfoxide ligands complementary to the three mentioned above (Scheme 6).

Under the same reaction conditions employed to obtain **16**, ligands **19**–**22** were synthesized in 65–85% overall yield. In all of these cases, the two expected atropisomers were separated and isolated after column chromatography alongside a third fraction that showed the (*DNHS*)-conformers at sulfur. Attempts to form the 4-(trifluoromethyl)phenyl derivative **23** using the lithiation path failed. We suppose that side reactions through *ortho*-metalation of the acidic proton in the 4-CF_3PhSO core are the reason for the complex mixture furnished by this experiment.[29] Nevertheless, **23** could be readily accessed when substituting the lithium nucleophile by its Grignard equivalent (78% yield). As described

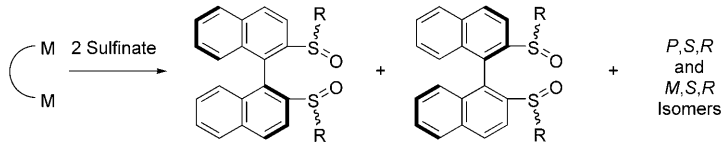

M = Li, MgBr

Sulfinate			
(*S*)-**10**	(*P*,*S*,*S*)-**19a** (18% yield)	(*M*,*S*,*S*)-**19c** (29% yield)	(*DNHS*)-**19b** (28% yield)
(*S*)-**11**	(*P*,*S*,*S*)-**20a** (30% yield)	(*M*,*S*,*S*)-**20c** (39% yield)	(*DNHS*)-**20b** (13% yield)
(*S*)-**12**	(*P*,*S*,*S*)-**21b** (30% yield)	(*M*,*S*,*S*)-**21c** (29% yield)	(*DNHS*)-**21a** (23% yield)
(*S*)-**14**	(*P*,*S*,*S*)-**22a** (31% yield)	(*M*,*S*,*S*)-**22c** (25% yield)	(*DNHS*)-**22b** (14% yield)
15	(*P*,*R*,*R*)-**23b** (48% yield)	---	(*DNHS*)-**23a** (29% yield)

Scheme 6. Variation of substituents on the sulfoxide moiety of *rac*-**1** derived ligands.

for **18**, the synthesis of **23** afforded the (*DNHS*)-conformer and only one of the two expected diastereoisomers.

To confirm the configurations at sulfur, at least one isomer of each of the disulfoxides **19**–**23** was characterized by X-ray diffraction studies (see the Supporting Information).[30] Analysis of their solid-state structures shows a gradual increase in the S–O bond lengths when going from the most electron-poor substituent at sulfur [**23b**, (1.483(2) Å)] to the most donating substituent [**21a** (1.4986(13) Å)]. In addition, the crystallographic studies carried out for **19b** [(*DNHS*)-Ph-BINASO] and **20b** [(*DNHS*)-4-FPh-BINASO] were the ultimate proof for the formation of non-homochiral diastereoisomers (Figure 3).

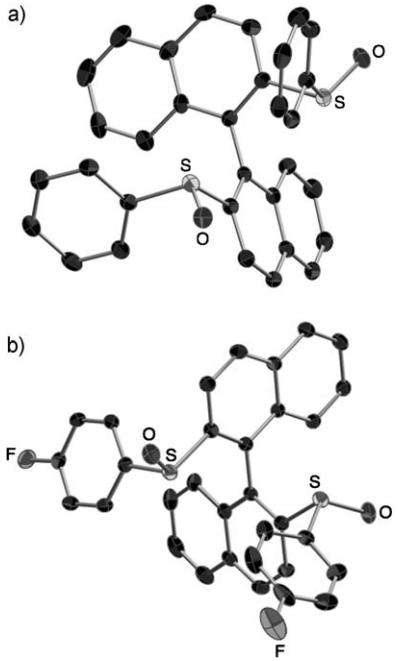

Figure 3. The solid-state molecular structures of a) (*DNHS*)-Ph-BINASO (**19b**) and b) (*DNHS*)-4-FPh-BINASO (**20b**).

Overall, the synthesis of the disulfoxide ligands by using consecutive nucleophilic substitutions at the two electrophilic sulfur moieties is certainly not as straightforward as we had expected. Although the generation of (*DNHS*)-conformers in some of these reactions is not entirely surprising, it does pose a serious problem for the unambiguous attribution of the stereochemistry of all of these compounds.

Reduction to disulfides and enantiomeric purity of ligands: The evidence for the presence of a (*DNHS*)-conformer in the synthesis of some of the ligands meant that we needed to find a means to ascertain the optical purity of our ligands. For instance, contamination of a given (*M*,*S*,*S*)-ligand with its (*P*,*R*,*R*)-enantiomer would spectroscopically go unnoticed. Initial, unsuccessful attempts were made by using chiral shift reagents and analyzing the mixture by ^{1}H NMR spectroscopy or by trying to analyze the very polar disulfoxide ligands by HPLC. Because of the conformational stability of the respective atropisomers (*M* and *P*), we realized that another straightforward method consisted of reducing both sulfoxides to the less polar sulfides and analyzing the products by HPLC. This path allows an indirect yet elegant determination of the purity of each homochiral diastereoisomers, as well as the (*DNHS*)-disulfoxides. By adapting literature procedures,[31] and by making sure that racemization of the atropisomeric backbone does not occur,[32] quantitative reduction of all disulfoxide ligand isomers gave their corresponding disulfides **24**–**31** (Scheme 7). Table 1 summarizes the HPLC results obtained for the respective disulfides and the isomeric purity of our disulfoxide ligands. The data reported validate all of the assumptions made above on

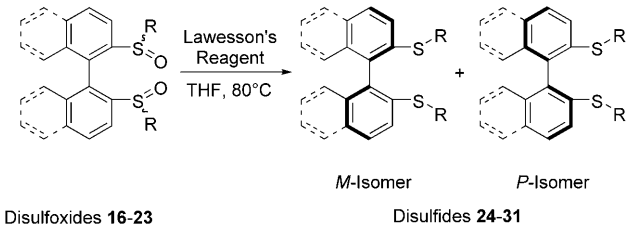

Scheme 7. Reduction of disulfoxides into disulfides using Lawesson's reagent.

Table 1. Enantiomeric excess of disulfides and corresponding disulfoxides.

Disulfide	*ee* [%][a]	Corresponding disulfoxide[b]
24	98	(*M*,*S*,*S*)-*p*-Tol-BINASO **16b**
	>99	(*P*,*S*,*S*)-*p*-Tol-BINASO **16a**
25	>99	(*M*,*R*,*R*)-*p*-Tol-MeBIPHESO **17a′**
	98	(*P*,*R*,*R*)-*p*-Tol-MeBIPHESO **17b′**
26	87	(*DNHS*)-*p*-Tol-H_8-BINASO **18a**
	>99	(*M*,*S*,*S*)-*p*-Tol-H_8-BINASO **18b**
27	95	(*P*,*S*,*S*)-Ph-BINASO **19a**
	39	(*DNHS*)-Ph-BINASO **19b**
	81	(*M*,*S*,*S*)-Ph-BINASO **19c**
28	96	(*P*,*S*,*S*)-4-FPh-BINASO **20a**
	0	(*DNHS*)-4-FPh-BINASO **20b**
	99	(*M*,*S*,*S*)-4-FPh-BINASO **20c**
29	nd[c]	(*DNHS*)-Cy-BINASO **21a**
	nd[c]	(*P*,*S*,*S*)-Cy-BINASO **21b**
	nd[c]	(*M*,*S*,*S*)-Cy-BINASO **21c**
30	96	(*P*,*S*,*S*)-4-MeOPh-BINASO **22a**
	60	(*DNHS*)-4-MeOPh-BINASO **22b**
	99	(*M*,*S*,*S*)-4-MeOPh-BINASO **22c**
31	55	(*DNHS*)-4-CF_3Ph-BINASO **23a**
	40	(*P*,*R*,*R*)-4-CF_3Ph-BINASO **23b**

[a] Enantiomeric excess determined by HPLC using ChiralPak-IB and Chiralcel OD-H columns. [b] Absolute configuration of the major isomer as assigned by crystallographic and catalytic results [(*M*,*S*,*S*)-(disulfoxide)-Rh gives (*R*)-**52aA** in the catalytic runs and (*P*,*R*,*R*)-(disulfoxide)-Rh gives (*S*)-**52aA**, reference 16]. [c] Not determined.

both the purities of the ligands and the starting sulfinates. The optical purity of the (*M*,*S*,*S*)- and (*P*,*S*,*S*)-pair of disulfoxides [or its equivalent (*M*,*R*,*R*)- and (*P*,*R*,*R*)-pair] corresponded at least to the initial optical purity of the sulfinates. In the case of the (*DNHS*)-isomers, we note that the distribution between the possible atropisomers varies from a perfectly racemic backbone (*DNHS*-**20b**) to one showing highly enriched atropisomeric distributions (*DNHS*-**18a**), adding another layer of complexity to the disulfoxide synthesis.

Synthesis of rhodium complexes: Two equivalents of ligands **16b**, **16b′**, **17b**, **17b′**, **18b**, **19c**, **20c**, **21c**, **22c**, and **23b** reacted cleanly with the rhodium ethylene dimer [{Rh(C_2H_4)$_2$Cl}$_2$] in dichloromethane to afford complexes **32**–**39** [{(disulfoxide)RhCl}$_2$] in very high yields after appropriate workup (Scheme 8, Table 2).[33]

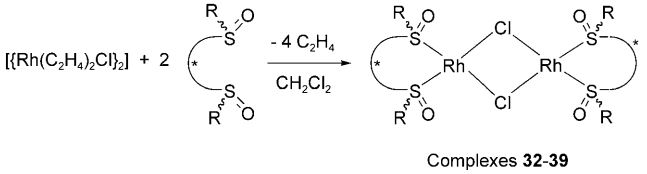

Scheme 8. Synthesis of dinuclear chloro-bridged rhodium complexes **32**–**39**.

Table 2. Ligands, corresponding rhodium complexes and isolated yields obtained.

Ligand	Complex	Yield [%]
(*P*,*R*,*R*)-*p*-Tol-BINASO (**16b′**)[a]	[{(**16b′**)RhCl}$_2$] (**32′**)	95
(*M*,*S*,*S*)-*p*-Tol-BINASO (**16b**)[a]	[{(**16b**)RhCl}$_2$] (**32**)	95
(*P*,*R*,*R*)-*p*-Tol-MeBIPHESO (**17b′**)[a]	[{(**17b′**)RhCl}$_2$] (**33′**)	93
(*M*,*S*,*S*)-*p*-Tol-MeBIPHESO (**17b**)[a]	[{(**17b**)RhCl}$_2$] (**33**)	95
(*M*,*S*,*S*)-*p*-Tol-H_8-BINASO (**18b**)	[{(**18b**)RhCl}$_2$] (**34**)	97
(*M*,*S*,*S*)-Ph-BINASO (**19c**)	[{(**19c**)RhCl}$_2$] (**35**)	99
(*M*,*S*,*S*)-4-FPh-BINASO (**20c**)	[{(**20c**)RhCl}$_2$] (**36**)	95
(*M*,*S*,*S*)-Cy-BINASO (**21c**)	[{(**21c**)RhCl}$_2$] (**37**)	96
(*M*,*S*,*S*)-4-MeOPh-BINASO (**22c**)	[{(**22c**)RhCl}$_2$] (**38**)	93
(*P*,*R*,*R*)-4-CF_3Ph-BINASO (**23b**)	[{(**23b**)RhCl}$_2$] (**39**)	93

[a] Values extracted from reference [16].

Binding of the sulfoxide ligands is accompanied by significant changes in the ^{1}H NMR spectra. An in situ reaction of **16b** with the rhodium precursor in CD_2Cl_2 showed fast displacement of the ethylene moieties by the disulfoxide. Crude reaction mixtures of **32**, **33**, and **38** were concentrated, layered with THF, and directly crystallized at low temperature to give analytically pure burgundy-colored material in high yield, as well as crystals suitable for X-ray diffraction studies. Compound **35** precipitated cleanly in dichloromethane upon completion of the reaction and crystals of complex **35** were, therefore, directly obtained by allowing a mixture of the rhodium precursor and ligand **19c** to react without stirring. Complexes **34**, **36**, **37**, and **39** were obtained as analytically pure products after precipitation with pentane and subsequent washings with diethyl ether and pentane.

The molecular structures of **32**, **33**, **35**, and **38** are displayed in Figure 4. The molecular structures of **32**, **33**, and **38** present the expected {Rh_2(-Cl)$_2$} butterfly shaped core, whereas complex **35** with the phenyl substituted ligand possesses an almost perfectly planar arrangement. Data of the most important bond lengths and angles for the disulfoxides **32**, **33**, **35**, and **38** and their analogous diphosphine complexes [({(*R*)-BINAP}RhCl)$_2$],[34] and [({(*S*)-BIPHEMP}RhCl)$_2$],[16b] are summarized in Tables S1 and S2 (see the Supporting Information).

Direct comparison of the disulfoxide and diphosphine complexes reveals ligand-donor–metal bond lengths that are very similar. Bite angles in the range of 97–98° were found for our disulfoxide complexes, whereas the phosphorus compounds present a slightly narrower bite angle at the metal (91–93°). In contrast, the dihedral angles of the atropisomeric backbones are very similar for the two ligand classes. Finally, coordination of the sulfoxide moiety to the metal leads to a shortening of the S=O bond, a phenomenon that gives a qualitative indication of the donor abilities of sulfoxides.

Rhodium carbonyl complexes and analysis of electron–donor properties: Correlation of the electron density on a metal with the $\nu_{(CO)}$ frequency of coordinated CO has been routinely used to evaluate the relative donor strength of various ligands in metal carbonyl complexes.[19b,35] To quantify to what extent our sulfoxide ligands are able to donate electron density to rhodium, we synthesized cationic carbonyl complexes of general formula [(L–L)Rh(CO)$_2$]$^+$ (where L–L is one of the investigated bidentate sulfoxide or analogous phosphine ligands) by treating [{Rh(CO)$_2$Cl}$_2$] with the chelating ligand in the presence of $AgBF_4$ (see the Supporting Information). IR spectroscopic data of these carbonyl complexes were collected and average carbonyl stretching frequencies are given in the right column of Table 3.

Analysis of Table 3, entries 1–3, reveals that substituting the fused aromatic rings of BINASO with sp^3-hybridized carbon atoms leads to an increase in electron-donation to

Table 3. Summary of IR spectroscopic data of cationic rhodium carbonyl complexes.

Entry	Complex	$\nu_{1(CO)}$[a]	$\nu_{2(CO)}$[a]	$\nu_{av(CO)}$[a,b]
1	[(**17b**)Rh(CO)$_2$]BF_4 (**41**)[c]	2100.10	2016.21	2058.16
2	[(**18b**)Rh(CO)$_2$]BF_4 (**42**)	2096.24	2023.93	2060.09
3	[(**16b**)Rh(CO)$_2$]BF_4 (**40**)[c]	2097.21	2025.85	2061.53
4	[(**21c**)Rh(CO)$_2$]BF_4 (**45**)	2091.42	2023.93	2057.68
5	[(**22c**)Rh(CO)$_2$]BF_4 (**46**)	2096.24	2023.93	2060.09
6	[(**16b**)Rh(CO)$_2$]BF_4 (**40**)[c]	2097.21	2025.85	2061.53
7	[(**19c**)Rh(CO)$_2$]BF_4 (**43**)	2098.17	2026.82	2062.50
8	[(**20c**)Rh(CO)$_2$]BF_4 (**44**)	2099.14	2026.82	2062.98
9	[(**23b**)Rh(CO)$_2$]BF_4 (**47**)	2102.03	2028.75	2065.39
10	[{(*rac*)-BINAP}Rh(CO)$_2$]BF_4 (**48**)[c]	2094.32	2048.89	2071.61
11	[{(*S*)-BIPHEMP}Rh(CO)$_2$]BF_4 (**49**)[c]	2094.32	2048.03	2071.18

[a] Values in cm^{-1}. [b] $\nu_{avarage(CO)} = (\nu_{1(CO)}\ [cm^{-1}] + \nu_{2(CO)}\ [cm^{-1}])/2$. [c] Values extracted from reference [16b].

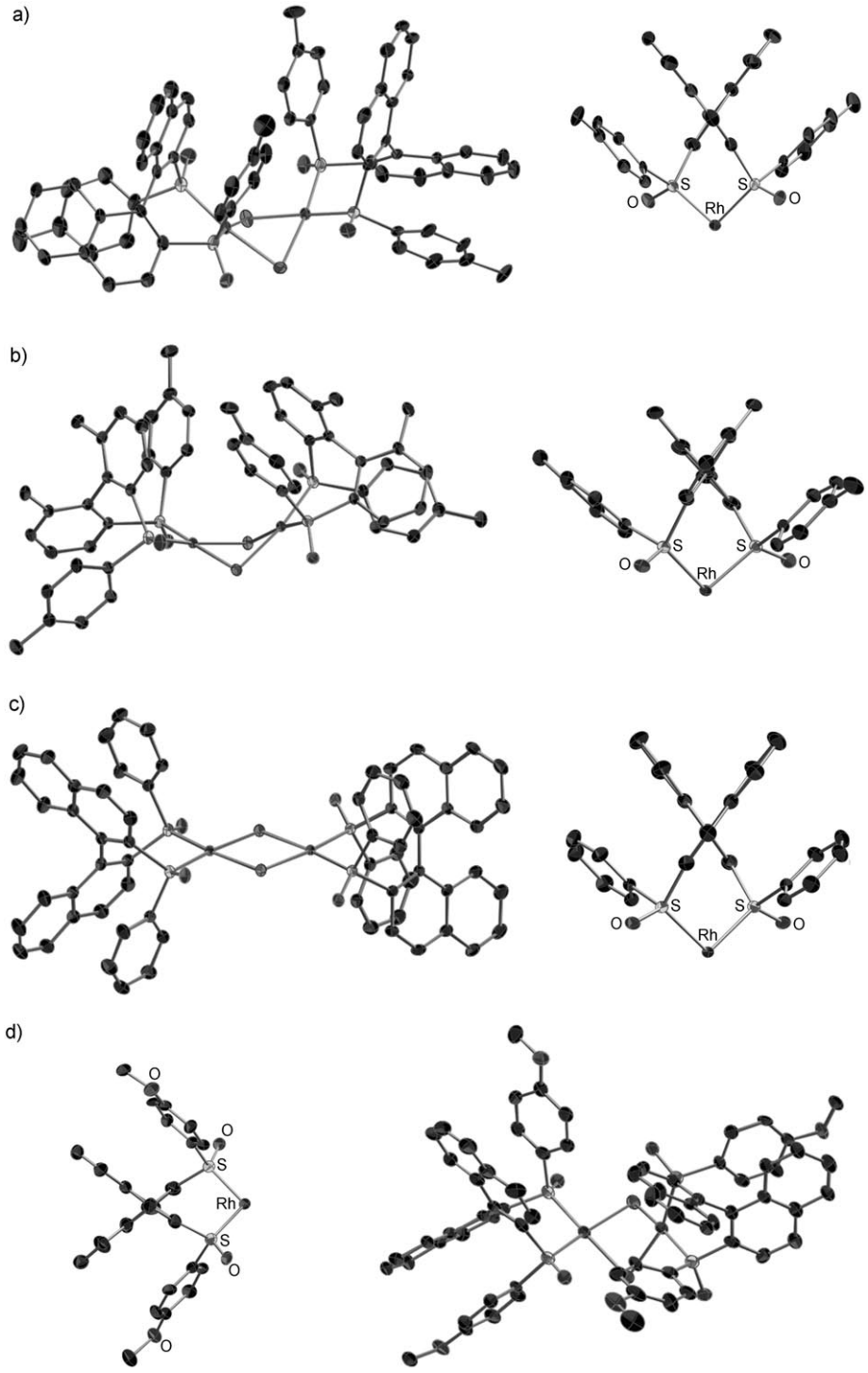

Figure 4. Full and half view of the solid-state molecular structures of complexes a) [{(*P*,*R*,*R*)-*p*-Tol-BINASO}RhCl]$_2$ (**32′**),[16a] b) [({(*M*,*S*,*S*)-*p*-Tol-MeBIPHESO}RhCl)$_2$] (**33**),[16b] c) [({(*M*,*S*,*S*)-Ph-BINASO}RhCl)$_2$] (**35**) and d) [({(*M*,*S*,*S*)-4-MeOPh-BINASO}RhCl)$_2$] (**38**).

the rhodium, as reflected by the decreasing stretching frequency observed in complexes **41** and **42**, as compared to **40**. That *p*-Tol-MeBIPHESO (complex **41**) shows stronger electron-donation than H_8-*p*-Tol-BINASO (complex **42**) likely indicates that the geometric factors of the backbone also influence the properties of the ligand. Likewise, varying the substitution on the sulfoxide moiety, while keeping the backbone unchanged (Table 3, entries 4–9), follows trends expected based on electronic arguments. The introduction of electron-withdrawing groups, such as fluorine and trifluoromethyl, in the *para* position of the phenyl ring of the sulfoxide leads to diminished electron density on the metal center (Table 3, entries 8, 9), whereas electron-donating groups (Table 3, entries 5, 6) or substitution of the aromatic moiety with a cyclohexyl group (Table 3, entry 4) increase the electron-density at rhodium.

Because the electronic characteristics of sulfoxides are largely unknown in the context of their coordination to metals and to understand how this ligand family compares to the parent diphosphines, we also synthesized and recorded the data for the corresponding [{(*rac*)-BINAP}Rh(CO)$_2$]BF$_4$ (**48**) and [{(*S*)-BIPHEMP}Rh(CO)$_2$]BF$_4$ (**49**) complexes (Table 3, entries 10, 11). Contrary to our initial expectations, the results demonstrate that our disulfoxides are more electron-donating than their diphosphine counterparts.[36,37]

Catalytic studies: We had previously established that precatalysts **32** and **33** performed very well in the Miyaura–Hayashi addition reaction of arylboronic acids to cyclic α,β-unsaturated substrates, surpassing BINAP and BIPHEMP ligands in both reactivity and selectivity. To understand the effects of electronic and steric variation of this first generation of chiral disulfoxide ligands in catalysis, we proceeded with the screening of the catalytic performances of complexes **32**–**39** in the standard 1,4-addition reaction of 2-cyclohexen-1-one (**50a**) and phenylboronic acid (**51A**). The results obtained are enclosed in Table 4.

Table 4. Catalytic results with complexes **32**–**39** in the coupling of **50a** with arylboronic acid **51A**.

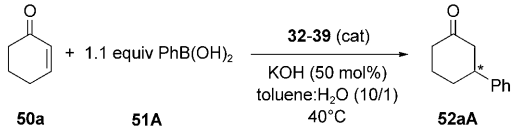

50a **51A** **52aA**

Entry	Complex	Conc. [mol%]	t [h][a]	Yield of **52aA** [%][b]	*ee* [%][c,d]
1	**32**	0.75	1	99	98 (*R*)
2	**32**	0.50	8	86	98 (*R*)
3	**32**	0.25	24	55	97 (*R*)
4	**33**	0.75	<0.5	98	>99 (*R*)
5	**33**	0.50	<0.5	99	>99 (*R*)
6	**33**	0.25	0.5	98	>99 (*R*)
7	**34**	0.75	<0.5	99	>99 (*R*)
8	**34**	0.50	<0.5	99	98 (*R*)
9	**34**	0.25	0.75	99	98 (*R*)
10	**35**	0.75	0.5	98	89 (*R*)
11	**35**	0.50	1	96	78 (*R*)
12	**35**	0.25	8	70	76 (*R*)
13	**36**	0.75	<0.5	97	>99 (*R*)
14	**36**	0.50	1	99	92 (*R*)
15	**36**	0.25	4	84	90 (*R*)
16	**37**	5.00	–	0	0
17	**38**	0.75	0.5	99	79 (*R*)
18	**38**	0.50	1.5	99	76 (*R*)
19	**38**	0.25	5	72	75 (*R*)
20	**39**	0.75	2	45	32 (*S*)
21	**39**	0.50	5	42	32 (*S*)
22	**39**	0.25	8	29	29 (*S*)

[a] Reaction is stopped after full conversion or when no further conversion is observed as determined by GC-MS. [b] Yield of isolated product after column chromatography. [c] Determined by HPLC analysis with Chiralcel OD-H: flow 0.5 mL min^{-1}, solvent Hexane/*i*PrOH 98:2. [d] Configuration of major isomer, determined by comparison with reported data.

Effects of backbone modification on reactivity and selectivity: There is a clear trend in both the reactivity and the selectivity of the reaction when changing the atropisomeric moiety of the disulfoxide ligands (Table 4, entries 1–9). The overall catalytic performance increases significantly when going from *p*-Tol-BINASO to its partially hydrogenated derivative *p*-Tol-H_8-BINASO, both in terms of reactivity and selectivity. Even better results (albeit only slightly) are observed with the *p*-Tol-MeBIPHESO ligand architecture. It is tempting to rationalize these findings on the basis of the IR stretching frequencies observed above for the rhodium–carbonyl complexes incorporating these ligands. It would, therefore, appear that decreasing the π acidity of the disulfoxide ligand backbone translates into increased reactivity in the 1,4-addition reaction. Nonetheless, interpreting the selectivity increase we observe for the same set of ligands is hampered by the fact that we were not able to crystallize complex **34**. In our view, this precludes a meaningful discussion of the steric effect (i.e., different dihedral angles of the backbones) on the selectivity of the reaction.[38]

Effects of sulfoxide modification on reactivity and selectivity: The modification of the *p*-Tolyl moiety of the parent *p*-Tol-BINASO ligand leads to marked differences in reactivity. Most strikingly, complex **37**, which contains the most σ-basic ligand of the binaphthyl series (cyclohexyl groups), is completely inactive towards the 1,4-addition of substrate **51A** to **50a** even at catalyst loadings of 5 mol% (Table 4, entry 16). Comparable effects have been reported with diphosphine ligands when going from aromatic to aliphatic substituents on phosphorus.[39] On the other side of our electronic spectrum, the *p*-CF_3Ph-derived ligand also leads to poor catalytic conversion (catalyst **39**). The other modifications result in precatalysts that show increased reactivity at 0.75 mol% catalyst loading when compared to the parent *p*-tolyl-substituted ligand **32**.

Selectivity differences may also be compared, albeit direct comparisons with **32** are only possible for the enantiomerically pure *p*-MeOPh-substituted (**38**, Table 4, entries 17–19) and the *p*-FPh-derived ligands (**36**, Table 4, entries 13–15). Precatalyst **38** shows a clear erosion of selectivity with a maximum of 79% *ee*. In contrast, complex **36** not only showed the best reactivity, but also produced product **52aA** with complete selectivity at 0.75 mol% catalyst loading (Table 4, entry 13).

Overall, the selectivities decrease for all of the precatalysts if catalyst loadings are too low to warrant a short reaction time to product **52aA**. If the results here are cumulative, it would also mean that combining the *p*-FPh-moiety of sulfinate (*S*)-**11** with the superior backbones of *rac*-**2** and *rac*-**3** could lead to optimized ligand structures for the present transformation.

Catalyst reactivity and selectivity path: Detailed research by Hayashi and co-workers on the asymmetric 1,4-addition reaction with BINAP-Rh has established the catalytic cycle shown in Scheme 9.[40] We have previously compared the activities of structurally related disulfoxide and diphosphine rhodium dimers with chloro and hydroxo bridges to study the reaction pathway (**A** in Scheme 9).[16b]

The study has shown that the diphosphine compounds are distinctly less active than the systems incorporating disulfoxides under the reaction conditions outlined in Table 4. It was also found that for diphosphine ligands, the transformation from the chloro-bridged dimer to the active species is clearly more difficult than formation of the monomeric [Rh]-OH species through dimer dissociation. The inverse trend was observed with our disulfoxide ligands for which the catalytic run performed by using the chloro-bridged dimers is faster and more efficient than starting with the corresponding [Rh]-OH dimer.[41] In addition to easier accessibility to the [Rh]-OH active species, the participation of the polarized oxygen atom of the sulfoxide in the transmetalation step might facilitate transfer of the aryl group to the rhodium (**B** of Scheme 9).[42]

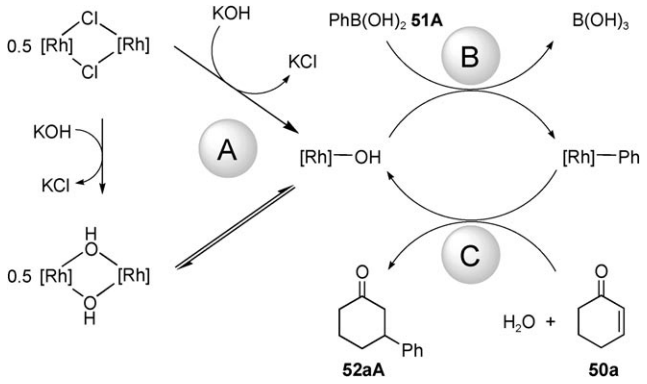

Scheme 9. Catalytic cycle for the rhodium catalyzed 1,4-additon of $PhB(OH)_2$ to 2-cyclohexen-1-one.

More intriguing than the higher reactivity of these disulfoxide ligands is their mode of action during the enantiodiscriminating step (**C** of Scheme 9). The stereochemical pathway in the Miyaura–Hayashi reaction catalyzed by BINAP, as well as in the overwhelming majority of metal-mediated asymmetric reactions, is based on the assumption that the substrates approach the metal so as to minimize steric interactions with the protruding R groups of the chiral ligand structure.[20,43] However, the half view of our rhodium disulfoxide complexes shown above (see partial views in Figure 4) clearly indicates that our system is devoid of any significant steric crowding around the metal center. Indeed, the aryl groups on the sulfoxide units are oriented away from the metal center and parallel to the atropisomeric backbone, leaving the oxygen atoms of the sulfoxide moieties as the sole entities approaching the metal center.

In-depth DFT computational studies were completed to allow us to gain insight into step **C** of the catalytic cycle of this reaction.[44] Notably, although the Miyaura–Hayashi reaction represents one of the most straightforward entries into useful chiral organic building blocks, and has emerged as an important methodology in organic synthesis, there have been very few computational studies to elucidate the pathway.[45]

The enantioselection step (step **C** of Scheme 9) begins with coordination of both enantiofaces of substrate **50a** to the [Rh]-Ph complex and proceeds without an energy barrier. The corresponding coordination intermediates display a distorted square planar (sp) geometry around the metal, see structures **53-sp-*R*** and **53-sp-*S*** in Figure 5 (*R* or *S* indicates that this complex will lead to the *R* or *S* enantiomer of **52aA**, respectively). In both structures the elongated C=C double bond of the substrate, 1.43 Å versus 1.34 Å in the uncoordinated **50a**, is almost perpendicular to the mean coordination plane around the metal center. In **53-sp-*R***, the cyclic part of the substrate is oriented away from the Rh–Ph group and towards one of the *p*-Tol groups, whereas in **53-sp-*S*** it is oriented right above the aromatic ring of the Rh–Ph group. Structure **53-sp-*R*** is only 0.2 kcal mol^{-1} more stable than **53-sp-*S***.

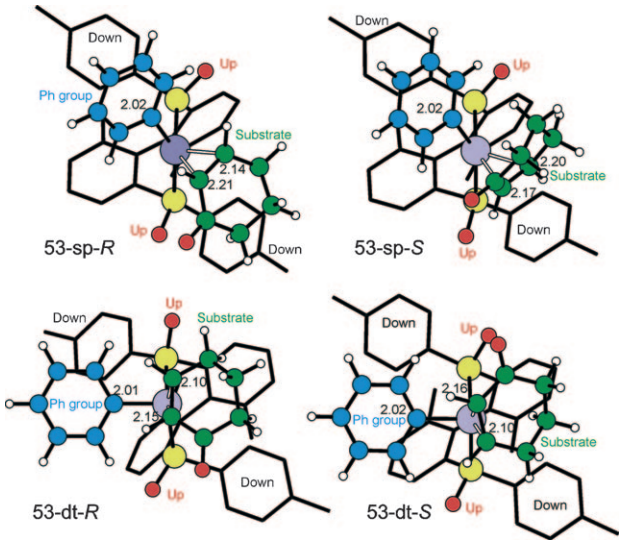

Figure 5. Structure and energy of the most stable square planar and distorted tetrahedral coordination intermediates. Bond lengths from the Rh atom to the centroid of the Ph group and to the coordinated C atoms of the substrate are also reported.

These coordination intermediates, however, can also assume a distorted tetrahedral (dt) geometry with the Ph group in the apical position, see structures **53-dt-*R*** and **53-dt-*S*** in Figure 5. In these structures the C=C double bond is rotated into a face of the tetrahedron, allowing for a somewhat higher back donation from the metal to the C=C double bond of the substrate, as evidenced by the elongation of 0.02 Å of the C=C double bond on going from the square-planar geometry to the distorted tetrahedral (1.43 Å in the sp geometries versus 1.45 Å in the dt geometries). The Rh–Ph bond length in the tetrahedral geometries is substantially unchanged relative to the square planar geometries, whereas the substrate is slightly closer to the metal.

These geometries are energetically competitive with the square planar analogues, since **53-dt-*R*** is only 0.9 kcal mol^{-1} higher in energy than **53-sp-*R***, whereas **53-dt-*S*** is 0.7 kcal mol^{-1} lower in energy than **53-sp-*S***. The conversion of the square planar geometries into the corresponding distorted tetrahedral is rather facile, with barriers of 5.4 and 6.8 kcal mol^{-1} for **53-sp-*R*** and **53-sp-*S***, respectively (the geometries of these transition states are reported in the Supporting Information). The substantially similar stability of the complexes, together with the low energy barriers for their interconversion, underline the remarkable manifold of structures available after substrate coordination, and that all these structures are probably in fast equilibrium. Although these results clearly pertain to a new ligand class, it is certainly interesting to observe that the initial binding of the olefin cannot represent the enantio-discriminating step in the reaction (this is commonly assumed for other ligand classes, such as chiral diphosphines or dienes).

Indeed, the stereoselective behavior of the present catalyst systems originates in the next catalytic step, namely the insertion of the C=C double bond of the substrate into the

Rh–Ph bond. The geometries of the transition states with the correct regiochemistry (labelled as **54-*R*** and **54-*S***) are shown in Figure 6.

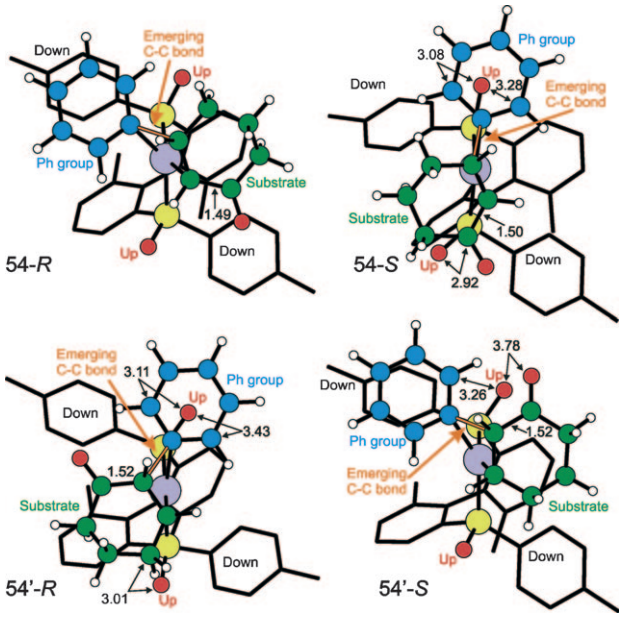

Figure 6. Structures of the transition states leading to formation of the *R* and *S* enantiomers of product **52aA** (distances in Å).

Transition state **54-*R*** deviates from planarity, with the C(Ph) atom lying out of the S-Rh-S plane by 1.23 Å, whereas in transition state **54-*S*** the C(Ph) atom is (or lies) only 0.03 Å out of the S-Rh-S plane. However, of greater importance is the fact that transition state **54-*R*** is favored over transition state **54-*S*** by 4.4 kcal mol^{-1}, which is in agreement with the experimental preferential formation of the *R* product with a (*P*,*S*,*S*) ligand. Analysis of the geometries of Figure 6 indicates clearly that the most favored **54-*R*** transition state presents both the Ph and the C=O group of the substrate in rather open parts of space, which is on the side of the *p*-tolyl rings that are bent away from the Rh atom. Instead, the competitive **54-*S*** transition state is disfavored by repulsive steric/electrostatic interactions between both the Ph and C=O groups of the substrate and the upward-pointing S=O groups of the ligand (see the short distances between these groups in Figure 6).

Concerning the transition states with the wrong regiochemistry (1,3-addition instead of 1,4-addition), in which the C2 atom of **50a** attacks the C(Ph) atom (labelled as **54′-*R*** and **54′-*S***), they are 9.7 and 5.2 kcal mol^{-1} higher in energy than **54-*R***, respectively. Both these transition states are higher in energy because formation of the C2–Ph bond decreases conjugation between the C2 atom and the C=O group more than formation of the C3–Ph bond, see the longer C2–CO distances in **54′-*R*** and **54′-*S*** relative to **54-*R***. In addition, **54′-*R*** is also destabilized by severe steric/electrostatic repulsion between the reacting groups and the ligand, see the short distances in Figure 6.

Focusing on the pathways corresponding to the correct regiochemistry, transition states **54-*R*** and **54-*S*** collapse into intermediates **55-*R*** and **55-*S*** shown in Figure 7. Intermedi-

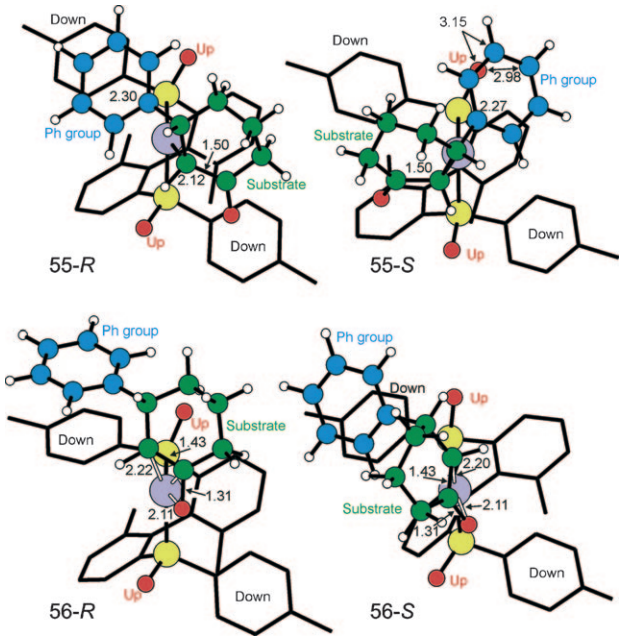

Figure 7. Structures of intermediates **55-*R*** and **55-*S***, and of intermediates **56-*R*** and **56-*S***, corresponding to the kinetic and to the thermodynamic products of insertion of an *R* and *S* coordinated substrate into the Rh–Ph bond.

ate **55-*R*** is more stable than the coordination intermediate **53-*R*** by 7.1 kcal mol^{-1}, whereas intermediate **55-*S*** is comparable in energy with the coordination intermediate **53-*S*** (0.2 kcal mol^{-1} higher in energy). In both intermediates the substrate wraps around the metal with the Ph group at least partially coordinated to the metal (average Rh···Ph distances in **55-*R*** and **55-*S*** are 2.30 Å). The instability of **55-*S*** can once again be explained by the repulsive interactions between one of the S=O groups and atoms of the Ph group (see the short distances in Figure 7). In contrast, in the most stable **55-*R*** intermediate the substrate is placed nicely away from the upwardly-pointing S=O groups. However, both intermediates **55-*R*** and **55-*S*** evolve toward the more stable **56-*R*** and **56-*S*** intermediates in which the C=O group displaces the Ph group from the metal, and an enolate-type structure η^3-coordinated to the metal through the C···C···O moiety is formed, see Figure 7. Intermediates **56-*R*** and **56-*S*** are more stable than **55-*R*** and **55-*S*** by 6.9 and 11.5 kcal mol^{-1}, respectively.

At this point, the missing step to complete step **C** of the catalytic cycle of Scheme 9 is an H transfer to break the Rh–C bond and to release the product. Considering that the reaction is performed in a 10:1 toluene/water mixture, we investigated if a water molecule can coordinate to the Rh atom of **56-*R*** and can transfer one of its protons to the substrate. Water coordination to **56-*R*** leads to **57-*R*** with an

energy gain of 10.1 kcal mol^{-1} (see Figure 8). After water coordination, the η^3-coordinated C···C···O moiety converts into an almost perfect enolate moiety with a well formed C=C bond not coordinated to the metal, and a short Rh–O-(enolate) σ-bond (Figure 8). The direct H transfer from the coordinated water molecule to the substrate proceeds through transition state **58-*R*** with the rather low barrier of 5.6 kcal mol^{-1}. In the transition state, the C=C enolate is almost completely transformed into a single C–C bond, whereas the enolate C–O bond is almost completely converted into a standard double C=O bond. In the final intermediate **59-*R***, which is more stable by 3.5 kcal mol^{-1} than **57-*R***, the product is coordinated to the metal through its C=O bond (Figure 8). Finally, reaction product **52aA** is released by simple dissociation of **52aA** from the metal with an energy release of 11.6 kcal mol^{-1} coordinating a water molecule, and finally regenerating the catalytically active monomeric [Rh]-OH species of Scheme 9.[46]

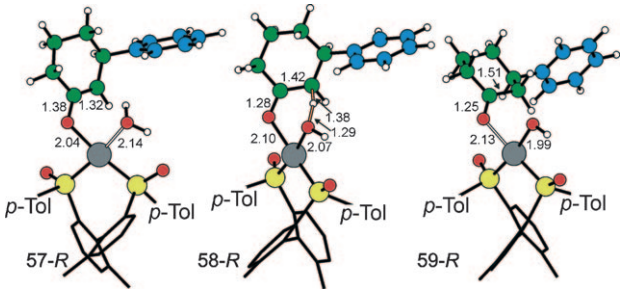

Figure 8. Relevant structures for water coordination and product release.

The energy profile corresponding to the favored reaction pathway leading to formation of the *R* product is shown in Figure 9. The plot clearly indicates that the first step, corresponding to insertion of the C=C bond of the 2-cyclohexen-1-one into the Rh–Ph bond of the square-planar **53-sp-*R*** complex is rate limiting. After insertion has occurred, rapid transformation of the resulting intermediate into the Rh complex **57-*R***, presenting the Rh-enolate bond and a coordinated water molecule, is achieved. Product release, through H-transfer from the coordinated water molecule of **57-*R*** to the C=C bond of the enolate bond, is an easy process that leads to the final complex **59-*R***, presenting the product coordinated to the Rh center through the re-established carbonyl functionality. The plot also shows why the product with the wrong stereochemistry is not observed, as the transition state **54-*S*** lies 4.4 kcal mol^{-1} higher in energy than the favored transition state **54-*R***. Finally, the starting complex can exist as an equilibrium between different isomers corresponding to square planar, **53-sp-*R***, and distorted tetrahedral, **53-dt-*R***, geometries, connected by a low energy isomerization barrier.

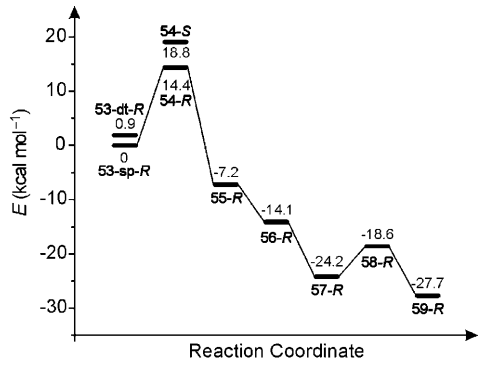

Figure 9. Energy profile corresponding to formation of the favored product (step **C** in Scheme 9). The energy of transition state **54-*S***, leading to the minor enantiomer, is also indicated.

Conclusion

We have introduced a new family of bidentate sulfoxide ligands with C_2-symmetric atropisomeric biaryl backbones. Combining optically pure or enriched sulfinate esters and racemic biaryl skeletons by using Andersen's methodology gave access to a series of sterically and electronically modified C_2-symmetric disulfoxides. Although the methodology used is well documented, a drawback, relating to the optical integrity of the ligands, was found by the detection, in some cases, of diastereoisomers possessing non-homochiral sulfur stereogenic centers. The reduction of the chiral sulfoxide moiety to achiral sulfides and HPLC analysis of the atropisomeric backbones has provided the necessary information on the purity of each isomer from the constituents of the family.

IR analysis of the electronic properties of the ligands through analysis of the carbonyl stretching frequencies of the corresponding [(disulfoxide)Rh(CO)$_2$]$^+$ complexes gave a clear picture on how different skeletons and sulfoxide substituents influence the donor/acceptor properties of the ligand family. The study indicates that a slightly more acidic character for the sulfoxide substituents and more electron-rich backbones provide catalytic systems with superior reactivity and selectivity in the 1,4-addition of phenylboronic acid to 2-cyclohexen-1-one. In addition, smaller R groups in the *para* position of the aromatic rings of the sulfoxide substituents and bulkier atropisomeric backbones are also increasing the catalytic performance.

Advanced DFT calculations have shown that the initial binding of the olefin is not the enantio-discriminating step (at least for the disulfoxide-based catalysts used here). Furthermore, the final protonation step involving the enolate-metal moiety follows a stepwise mechanism whereby initial binding of a water molecule to the rhodium center precedes an intramolecular protonation and release mechanism of the enolate. Calculations on the reaction path have also uncovered the mechanism by which these disulfoxide–rhodium catalysts discriminate between the two possible enantiomeric products. Contrary to more traditional chiral ligand frameworks, electronic factors arising from the sulfoxide moiety seem to be, at least, partially responsible for the high

enantioselectivities observed in catalysis. These findings should prove useful for future research in the use of sulfoxide based ligands, allowing a rational design of structures that take advantage of the phenomenon described here.

Experimental Section

All computational and experimental details can be found in the Supporting Information.

CCDC-781539–781553 contain the supplementary crystallographic data for this paper (see Supporting Information for further details. These data can be obtained free of charge from The Cambridge Crystallographic Data Centre via www.ccdc.cam.ac.uk/data_request/cif. The Crystallographic data for compounds **16a′**, **17b**, **32** and **33** have been published elsewhere.[16]

Acknowledgements

R.D. holds an Alfred Werner Assistant Professorship and thanks the foundation for generous financial support. R.M. thanks the Swiss National Science Foundation (SNF) and E.D. thanks the Roche Research Foundation (RRF) for support. A.P. is grateful for the allocation of a Ramón y Cajal contract by the Spanish MEC. L.C. thanks the HPC team of Enea (www.enea.it) for using the ENEA-GRID and the HPC facilities CRESCO (www.cresco.enea.it) in Portici, Italy.

[1] a) *Asymmetric Catalysis in Organic Synthesis* (Ed.: R. Noyori), Wiley, New York, **1994**; b) *Catalytic Asymmetric Synthesis II* (Ed.: Ojima), Wiley, New York, **2000**; c) *Comprehensive Asymmetric Catalysis* (Eds.: E. N. Jacobsen, A. Pfaltz, H. Yamamoto), Springer, Berlin, **1999**; d) H. U. Blaser, F. Spindler, M. Studer, *Appl. Catal. A* **2001**, *221*, 119.

[2] a) S. C. Stinson, *Chem. Eng. News* **1992**, *70*, 46; b) S. C. Stinson, *Chem. Eng. News* **2001**, *79*, 45; c) S. Borman, *Chem. Eng. News* **1990**, *68*, 9.

[3] a) J. K. Whitesell, *Chem. Rev.* **1989**, *89*, 1581; b) A. Pfenninger, *Synthesis* **1986**, 89; c) R. Noyori, I. Tomino, M. Yamada, M. Nishixawa, *J. Am. Chem. Soc.* **1984**, *106*, 6709; d) T. R. Kelly, A. Whiting, N. S. Chandrakumar, *J. Am. Chem. Soc.* **1986**, *108*, 3510; e) K. Narasaka, M. Inoue, N. Okada, *Chem. Lett.* **1986**, 1109; f) E. J. Corey, N. Imai, H.-Y. Zhang, *J. Am. Chem. Soc.* **1991**, *113*, 728; g) D. A. Evans, K. A. Woerpel, M. M. Hinman, M. M. Faul, *J. Am. Chem. Soc.* **1991**, *113*, 726; h) R. E. Lowenthal, A. Abiko, S. Masamune, *Tetrahedron Lett.* **1990**, *31*, 6005.

[4] For an excellent recent review on the use of chiral olefin containing ligands, see: a) C. Defieber, H. Grützmacher, E. M. Carreira, *Angew. Chem.* **2008**, *120*, 4558; *Angew. Chem. Int. Ed.* **2008**, *47*, 4482. For selected references, see: b) T. Hayashi, K. Ueyama, N. Tokunaga, K. Yoshida, *J. Am. Chem. Soc.* **2003**, *125*, 11508; c) N. Tokunaga, Y. Otomaru, K. Okamoto, K. Ueyama, S. Shintani, T. Hayashi, *J. Am. Chem. Soc.* **2004**, *126*, 13584; d) R. Shintani, K. Okamoto, Y. Otomaru, K. Ueyama, T. Hayashi, *J. Am. Chem. Soc.* **2005**, *127*, 54; e) C. Fischer, C. Defieber, T. Suzuki, E. M. Carreira, *J. Am. Chem. Soc.* **2004**, *126*, 1628; f) C. Defieber, J.-F. Paquin, S. Serna, E. M. Carreira, *Org. Lett.* **2004**, *6*, 3873; g) J.-F. Paquin, C. R. J. Stephenson, C. Defieber, E. M. Carreira, *Org. Lett.* **2005**, *7*, 3821; h) J.-F. Paquin, C. Defieber, C. R. J. Stephenson, E. M. Carreira, *J. Am. Chem. Soc.* **2005**, *127*, 10850.

[5] a) M. Calligaris, O. Carugo, *Coord. Chem. Rev.* **1996**, *153*, 83; b) J. C. Bayón, C. Claver, A. M. Masdeu-Bultó, *Coord. Chem. Rev.* **1999**, *193*, 73; c) I. Fernández, N. Khiar, *Chem. Rev.* **2003**, *103*, 3651.

[6] a) D. R. Rayner, A. J. Gordon, K. Mislow, *J. Am. Chem. Soc.* **1968**, *90*, 4854; b) K. Mislow, J. Siegel, *J. Am. Chem. Soc.* **1984**, *106*, 3319.

[7] a) A. J. Walker, *Tetrahedron: Asymmetry* **1992**, *3*, 961; b) G. Solladie, M. C. Carrefio in *Organosulphur Chemistry, Synthetic Aspects*, Academic Press, New York, **1995**; c) G. H. Posner in *The Chemistry of Sulfones and Sulfoxides*, Wiley, New York, **1988**; d) G. H. Posner, *Acc. Chem. Res.* **1987**, *20*, 72; e) M. C. Carreño, *Chem. Rev.* **1995**, *95*, 1717.

[8] For achiral catalysis with sulfoxide ligands, see: a) Y. M. Y. Haddad, H. B. Henbest, J. Husbands, T. R. B. Mitchell, J. Trocha-Grimshaw, *J. Chem. Soc. Perkin Trans. 1* **1974**, 596; b) B. R. James, R. H. Morris, *J. Chem. Soc. Chem. Commun.* **1978**, 929; c) A. Greenberg, A. Gogoll, J.-E. Backvall, *J. Org. Chem.* **1991**, *56*, 5808; d) R. C. Larock, R. Hightower, L. A. Hasvold, K. P. Peterson, *J. Org. Chem.* **1996**, *61*, 3584; e) M. S. Chen, M. C. White, *J. Am. Chem. Soc.* **2004**, *126*, 1346; f) K. J. Fraunhoffer, N. Prabagaran, L. E. Sirois, M. C. White, *J. Am. Chem. Soc.* **2006**, *128*, 9032.

[9] For attempts showing low selectivities/reactivities: a) B. R. James, R. S. McMillan, *Can. J. Chem.* **1977**, *55*, 3927; b) N. Khiar, I. Fernandez, F. Alcudia, *Tetrahedron Lett.* **1993**, *34*, 123; c) R. Tokunoh, M. Sodeoka, K. Aoe, M. Shibasaki, *Tetrahedron Lett.* **1995**, *36*, 8035. For two very recent examples of high enantioselectivity using disulfoxide ligands, see: d) Q.-A. Chen, X. Dong, M.-W. Chen, D.-S. Wang, Y.-G. Zhou, Y.-X. Li, *Org. Lett.* **2010**, *12*, 1928; e) J. Chen, J. Chen, F. Lang, X. Zhang, L. Cun, J. Zhu, J. Deng, J. Liao, *J. Am. Chem. Soc.* **2010**, *132*, 4552.

[10] For better reactivities and selectivities using sulfoxide/nitrogen or sulfoxide/phosphine chelates, see: a) J. V. Allen, J. F. Bower, J. M. J. Williams, *Tetrahedron: Asymmetry* **1994**, *5*, 1895; b) K. Hiroi, Y. Suzuki, *Tetrahedron Lett.* **1998**, *39*, 6499; c) K. Hiroi, Y. Suzuki, I. Abe, Y. Hasegawa, K. Suzuki, *Tetrahedron: Asymmetry* **1998**, *9*, 3797; d) D. G. I. Petra, P. C. J. Kamer, A. L. Spek, H. E. Schoemaker, P. W. N. M. van Leeuwen, *J. Org. Chem.* **2000**, *65*, 3010; e) K. Hiroi, Y. Suzuki, I. Abe, R. Kawagishi, *Tetrahedron* **2000**, *56*, 4701; f) K. Hiroi, I. Izawa, T. Takizawa, K. Kawai, *Tetrahedron* **2004**, *60*, 2155; g) J. Chen, D. Li, H. Ma, L. Cun, J. Zhu, J. Deng, J. Liao, *Tetrahedron Lett.* **2008**, *49*, 6921; h) J. Chen, F. Lang, D. Li, L. Cun, J. Zhu, J. Deng, J. Liao, *Tetrahedron: Asymmetry* **2009**, *20*, 1953; i) F. Lang, D. Li, J. Chen, J. Chen, L. Li, L. Cu, J. Zhu, J. Deng, J. Liao, *Adv. Synth. Catal.* **2010**, *352*, 843.

[11] a) K. K. Andersen, W. Gaffield, N. E. Papanikolaou, J. W. Foley, R. I. Perkins, *J. Am. Chem. Soc.* **1964**, *86*, 5637; b) K. K. Andersen, *Int. J. Sulfur Chem., Part B* **1971**, *6*, 69; c) C. Mioskowski, G. Solladié, *Tetrahedron* **1980**, *36*, 227; d) C. Mioskowski, G. Solladié, *Tetrahedron Lett.* **1975**, *16*, 3341; e) G. Solladié, J. Hutt, A. Girardin, *Synthesis* **1987**, 173; f) S. C. Benson, J. K. Snider, *Tetrahedron Lett.* **1991**, *32*, 5885; g) F. Rebiere, O. Samuel, L. Ricard, H. B. Kagan, *J. Org. Chem.* **1991**, *56*, 5991; h) J. K. Whitesell, M.-S. Wong, *J. Org. Chem.* **1991**, *56*, 4552; i) D. A. Evans, M. M. Faul, L. Colombo, J. J. Bisaha, J. Clardy, D. Cherry, *J. Am. Chem. Soc.* **1992**, *114*, 5977; j) W. Oppolzer, *Pure Appl. Chem.* **1990**, *62*, 1241; k) I. Fernández, N. Khiar, J. M. Llera, F. Alcudia, *J. Org. Chem.* **1992**, *57*, 6789.

[12] a) J. Clayden, P. M. Kubinski, F. Sammiceli, M. Helliwell, L. Diorazio, *Tetrahedron* **2004**, *60*, 4387; b) F. García-Flores, L. S. Flores-Michel, E. Juaristi, *Tetrahedron Lett.* **2006**, *47*, 8235.

[13] T. Thaler, F. Geittner, P. Knochel, *Synlett* **2007**, 2655.

[14] a) A. Miyashita, A. Yasuda, H. Takaya, K. Toriumi, T. Ito, T. Souchi, R. Noyori, *J. Am. Chem. Soc.* **1980**, *102*, 7932; b) H. Takaya, K. Mashima, K. Koyano, M. Yagi, H. Kumobayashi, T. Taketomi, S. Akutagawa, R. Noyori, *J. Org. Chem.* **1986**, *51*, 629.

[15] R. Schmid, M. Cereghetti, B. Heiser, P. Schönholzer, H.-J. Hansen, *Helv. Chim. Acta* **1988**, *71*, 897.

[16] a) R. Mariz, X. Luan, M. Gatti, A. Linden, R. Dorta, *J. Am. Chem. Soc.* **2008**, *130*, 2172; b) J. J. Bürgi, R. Mariz, M. Gatti, E. Drinkel, X. Luan, S. Blumentritt, A. Linden, R. Dorta, *Angew. Chem.* **2009**, *121*, 2806; *Angew. Chem. Int. Ed.* **2009**, *48*, 2768.

[17] H. Shimizu, I. Nagasaki, T. Saito, *Tetrahedron* **2005**, *61*, 5405.

[18] Z. Freixa, P. W. N. M. van Leeuwen, *Dalton Trans.* **2003**, 1890.

[19] a) K. Mashima, K.-H. Kusano, N. Sato, Y.-I. Matsumura, K. Nozaki, H. Kumobayashi, N. Sayo, Y. Hori, T. Ishizaki, S. Akutagawa, H. Takaya, *J. Chem. Soc. Chem. Commun.* **1991**, 609; b) K. Mashima,

K. Kusano, N. Sato, Y. Matsumura, K. Nozaki, H. Kumobayashi, N. Sayo, Y. Hori, T. Ishizaki, S. Akutagawa, H. Takaya, *J. Org. Chem.* **1994**, *59*, 3064.

[20] For the proposed selectivity pathway in the original BINAP–Rh^{I} system, see: a) Y. Takaya, M. Ogasawara, T. Hayashi, M. Sakai, N. Miyaura, *J. Am. Chem. Soc.* **1998**, *120*, 5579. For a review on the rhodium-catalyzed 1,4-addition: b) T. Hayashi, K. Yamasaki, *Chem. Rev.* **2003**, *103*, 2829.

[21] A. Poater, F. Ragone, R. Mariz, R. Dorta, L. Cavallo, *Chem. Eur. J.* **2010**, *16*, 14348.

[22] Comopund *rac*-**3** is reasonably priced when purchased in >100 g quantities from Dalchem/ABCR ($<10$$/g). Alternatively, it can be prepared in good quantities from the corresponding alcohol, see: A. Miyashita, H. Takaya, T. Souchi, R. Noyori, *Tetrahedron* **1984**, *40*, 1245.

[23] a) G. Svensson, J. Albertsson, T. Frejd, T. Klingsted, *Acta Crystallogr.* **1986**, *C42*, 1324; b) Y. Liang, S. Gao, H. Wan, J. Wang, H. Chen, Z. Zheng, X. Hu, *Tetrahedron: Asymmetry* **2003**, *14*, 1267; see also reference [15a].

[24] For synthesis and structural features of its diphosphine counterpart, see: a) N. Sayo, H. Kumobayashi EP 479 542, **1992**; [*Chem. Abstr.* **1992**, *117*, 111803]; b) X. Zhang, K. Mashima, K. Koyano, N. Sayo, H. Kumobayashi, S. Akutagawa, H. Takaya, *Tetrahedron Lett.* **1991**, *32*, 7283; c) X. Zhang, K. Mashima, K. Koyano, N. Sayo, H. Kumobayashi, S. Akutagawa, H. J. Takaya, *Chem. Soc. Perkin Trans. 1* **1994**, 2309.

[25] a) C. Alayrac, S. Nowaczyk, M. Lemarié, P. Metzner, *Synthesis* **1999**, 669. For X-ray analysis see: b) C. Alayrac, J.-F. Saint-Clair, M. Lemarié, P. Metzner, M.-T. Averbuch-Pouchot, *Acta Crystallogr. Sect. A* **1999**, *55*, 262.

[26] Both (1*R*,2*S*,5*R*)-(−)-menthyl (*S*)-*p*-toluenesulfinate and (1*S*,2*R*,5*S*)-(+)-menthyl (*R*)-*p*-toluenesulfinate can be purchased in high *de* ratio from various chemical suppliers.

[27] J. M. Klunder, K. B. Sharpless, *J. Org. Chem.* **1987**, *52*, 2598.

[28] The protocol reported in the Supporting Information of this manuscript gives superior yields of *p*-Tol-BINASO compared to the procedures given in reference [12a] and reference [16a].

[29] *Ortho*-metallation of sulfoxides is well-documented and sometimes directs the reaction outcome to undesired products, for example: R. J. Kloetzing, P. Knochel, *Tetrahedron: Asymmetry* **2006**, *17*, 116.

[30] The crystal structures of ligands **19a** and **19c** show that these compounds are not enantiopure as expected (see purity of starting sulfinate **10**). The major isomer was determined indirectly by HPLC and the catalytic results (see: reduction to disulfides and enantiomeric purity of ligands) to have the *S*,*S*-configuration at the sulfur centers. Likewise, ligand **23b** contains the *R*,*R*-configured isomer as the major component.

[31] a) H. Bartsch, T. Erker, *Tetrahedron Lett.* **1992**, *33*, 199; b) N. Tewari, Y. Kumar, R. K. Thaper, J. M. Khanna, *Synth. Commun.* **1996**, *26*, 1169; c) K. Shimada, K. Kodaki, S. Aoyagi, Y. Takikawa, C. Kabuto, *Chem. Lett.* **1999**, 695; d) A. Ishii, R. Yamashita, M. Saito, J. Nakayama, *J. Org. Chem.* **2003**, *68*, 1555; e) D. K. Bates, X. Li, P. V. Jog, *J. Org. Chem.* **2004**, *69*, 2750.

[32] The disulfides **24**–**31** were subjected to identical reaction conditions as for their synthesis using elevated temperatures (up to 100 °C) and extended reaction times (up to 2 days). No change in enantiomeric ratios was found as determined by HPLC analysis.

[33] The other isomers of ligands **16**–**23** did not form clean complexes of the corresponding dimers and (*DNHS*)-conformers of the ligands were not used in our study. Our hypothesis is that steric repulsion from the sulfoxide groups hinders formation of the bridged complexes, a phenomenon that was also observed for atropisomeric diphosphine ligands incorporating bulky aromatic groups on phosphorus atoms, see: T. Ohshima, H. Tadaoka, K. Hori, N. Sayo, K. Mashima, *Chem. Eur. J.* **2008**, *14*, 2060.

[34] K. A. Bunten, D. H. Farrar, A. J. Poe, A. Lough, *Organometallics* **2002**, *21*, 3344.

[35] In the case of Rh^{I} complexes, donor–acceptor properties of diphosphines have been investigated by studying the carbonyl stretching frequencies of [(diphosphine)RhCl(CO)] compounds, see: a) L. Vallarino, *J. Chem. Soc.* **1957**, 2287; b) W. Hieber, R. Kummer, *Chem. Ber.* **1967**, *100*, 148; c) A. R. Sanger, *J. Chem. Soc. Dalton Trans.* **1977**, 120; d) S. Jeulin, S. Duprat de Paule, V. Ratovelomanana-Vidal, J.-P. Genêt, N. Champion, P. Dellis, *Angew. Chem.* **2004**, *116*, 324; *Angew. Chem. Int. Ed.* **2004**, *43*, 320; e) D. E. Kim, C. Choi, I. S. Kim, S. Jeulin, V. Ratovelomanana-Vidal, J.-P. Genêt, N. Jeong, *Adv. Synth. Catal.* **2007**, *349*, 1999.

[36] The differences in average stretching frequencies are big enough to exclude misinterpretation, owing to different bite angles (and resulting geometry/orbital overlap differences) between the complexes. For stretching frequencies of other rhodium-dicarbonyl complexes with chelating diphosphine ligands, see, for example: T. A. Betley, J. C. Peters, *Angew. Chem.* **2003**, *115*, 2487; *Angew. Chem. Int. Ed.* **2003**, *42*, 2385.

[37] Such a direct comparison of different ligand families can be misleading. The data obtained here do not imply that the disulfoxide ligands are binding more tightly to Rh^{I} than diphosphines, but merely reflect the relative contributions of donor and accepting properties of different ligand families. For a recent computational analysis on the subject, see: D. G. Gusev, *Organometallics* **2009**, *28*, 763.

[38] For discussions on the effect of dihedral angles on selectivity and reactivity, see for example: a) X. Zhang, T. Taketomi, T. Yoshizumi, H. Kumobayashi, S. Akutagawa, K. Mashima, H. Takaya, *J. Am. Chem. Soc.* **1993**, *115*, 3318; b) T. Uemura, X. Zhang, K. Matsumura, N. Sayo, H. Kumobayashi, T. Ohta, K. Nozaki, H. Takaya, *J. Org. Chem.* **1996**, *61*, 5510; c) T. Shinohara, K. Kondo, H. Ogawa, T. Mori, K. Nozaki, T. Hiyama, *Chirality* **2000**, *12*, 425.

[39] T. Shibata, H. Tsuruta, H. Danjo, T. Imamoto, *J. Mol. Catal. A* **2003**, *196*, 117.

[40] a) T. Hayashi, M. Takahashi, Y. Takaya, *J. Am. Chem. Soc.* **2002**, *124*, 5052; b) A. Kina, H. Iwamura, T. Hayashi, *J. Am. Chem. Soc.* **2006**, *128*, 3904.

[41] A recent report on the use of modified atropisomeric diphosphines as ligands for rhodium-catalyzed 1,4-addition in toluene/water has come to similar conclusions, see: T. Korenaga, K. Osaki, R. Maenishi, T. Sakai, *Org. Lett.* **2009**, *11*, 2325.

[42] A similar effect has been proposed for conjugated additions with rhodium quinonoid catalysts, see: a) U. S. Son, S. B. Kim, J. A. Reingold, G. B. Carpenter, D. A. Sweigart, *J. Am. Chem. Soc.* **2005**, *127*, 12238; b) W. C. Trenkle, J. L. Barkin, S. U. Son, D. A. Sweigart, *Organometallics* **2006**, *25*, 3548.

[43] K. E. Koenig, M. J. Sabacky, G. L. Bachman, W. C. Christopfel, H. D. Barnstorff, R. B. Friedman, W. S. Knowles, B. R. Stults, B. D. Vineyard, D. J. Weinkauff, *Ann. N. Y. Acad. Sci.* **1980**, *333*, 16.

[44] Details of DFT calculations are included in the Supporting Information.

[45] a) T. Itoh, T. Mase, T. Nishikata, T. Iyama, H. Tachikawa, Y. Kobayashi, Y. Yamamoto, N. Miyaura, *Tetrahedron* **2006**, *62*, 9610. For DFT calculations on a related 1,4-addition–enantioselective protonation reaction, see: b) L. Navarre, R. Martinez, J.-P. Genet, S. Darses, *J. Am. Chem. Soc.* **2008**, *130*, 6159.

[46] We also tested if the H-transfer from the coordinated water molecule of **57-*R*** could follow a two-step pathway, in which the H is first transferred to the Rh with formation of a Rh-hydride species (oxidative addition of water) followed by reductive elimination of the substrate. The H-transfer to the metal has a barrier of 25.3 kcal mol^{-1}, which is 19.7 kcal mol^{-1} higher than the barrier for the direct transfer from the water molecule to the substrate, supporting the low energy mechanism pathway shown in Figure 8.

Received: June 21, 2010
Published online: November 12, 2010

